

1 **Discovery of viral myosin genes with complex**
2 **evolutionary history within plankton**
3
4

5 Soichiro Kijima,¹ Tom O. Delmont,² Urara Miyazaki,^{1,3} Morgan Gaia,²
6 Hisashi Endo,¹ and Hiroyuki Ogata^{1,*}
7

8 ¹Institute for Chemical Research, Kyoto University, Gokasho, Uji, Kyoto 611-0011, Japan

9 ²Metabolic Genomics, Genoscope, Institut de Biologie François Jacob, CEA, CNRS, Univ
10 Evry, Université Paris Saclay, 91000 Evry, France

11 ³Laboratory of Marine Environmental Microbiology, Division of Applied Biosciences,
12 Graduate School of Agriculture, Kyoto University, Kitashirakawa-Oiwakecho, Sakyo-ku,
13 Kyoto, Kyoto 606-8502, Japan

14 * Corresponding author: E-mail: ogata@kuicr.kyoto-u.ac.jp

15 **Abstract**

16 Nucleocytoplasmic large DNA viruses (NCLDVs) infect diverse eukaryotes and form a
17 group of viruses with capsids encapsulating large genomes. Recent studies are increasingly
18 revealing a spectacular array of functions encoded in their genomes, including genes for
19 energy metabolisms, nutrient uptake, as well as cytoskeleton. Here, we report the discovery
20 of genes homologous to myosins, the major eukaryotic motor proteins previously
21 unrecognized in the virosphere, in environmental genomes of NCLDVs from the surface
22 of the oceans. Interestingly, these genes were often accompanied by kinesin genes in the
23 environmental genomes, suggesting a role of these viral proteins in the intracellular viral
24 particle transport. Phylogenetic analyses indicate that most viral myosins (named
25 “virmyosins”) belong to the *Imitervirales* order, except for one belonging to the
26 *Phycodnaviridae* family. On the one hand, the phylogenetic positions of virmyosin-
27 encoding *Imitervirales* are scattered within the *Imitervirales*. On the other hand,
28 *Imitervirales* virmyosin genes form a monophyletic group in the phylogeny of diverse
29 myosin sequences. Furthermore, phylogenetic trends for the virmyosin genes and viruses
30 containing them were incongruent. Based on these results, we argue that multiple transfers
31 of myosin homologs have occurred not only from eukaryotes to viruses but also between
32 viruses, supposedly during co-infections of the same host.

33 INTRODUCTION

34 Viruses were considered as tiny and simple biological objects until La Scola et al.
35 discovered a giant virus from the water of a cooling tower in 2003 (Scola et al., 2003). The
36 virus named mimivirus is 750 nm in particle size and possesses a 1,182 kbp genome
37 (Colson et al., 2017), a dimension that was large and complex enough to blow off the
38 classical perception of viruses. After the discovery of mimivirus, related viruses were
39 isolated including marseilleviruses, pandoraviruses, and pithoviruses, many of them with
40 similar or even larger-sized particles or genomes (Abergel et al., 2015; Colson et al., 2017).
41 These giant viruses infect diverse eukaryotes, possess a double-stranded DNA genome,
42 belong to the phylum *Nucleocytoplasmicota* (Koonin et al., 2020), and are commonly referred
43 to as nucleocytoplasmic large DNA viruses (NCLDVs) (Iyer et al., 2006). The
44 monophyletic origin of NCLDVs has been suggested based on the presence of about 40
45 core genes of NCLDVs that can be traced back to their putative last common ancestor
46 (Koonin and Yutin, 2019) as well as the congruent phylogenies of the most conserved 8
47 proteins responsible for virion morphogenesis and informational processes (Guglielmini
48 et al., 2019).

49 Because of their large virions, NCLDVs can encapsulate a large genome (several
50 hundred kb up to 2.5 Mb) in their particles. Smaller viruses (such as small RNA viruses)
51 encode only genes that are essential for their genome replication and capsid formation,
52 whilst NCLDVs encode numerous genes that are not directly involved in their genome
53 replication and virion morphogenesis (Moniruzzaman et al., 2020). These genes, often
54 called auxiliary metabolic genes, are considered to function in reprogramming host
55 metabolism and molecular machinery during viral infection towards enhancing viral
56 replication and subsequent transmission to another host. For example, the recently
57 characterized *Prymnesium kappa* virus RF01 encodes genes for all four succinate
58 dehydrogenase subunits, as well as genes for modulating β -oxidation pathway (Blanc-
59 Mathieu et al., 2021). These viral genes are suggested to boost energy production during
60 viral replication, which can deteriorate host metabolism, or to enhance the supply of
61 building blocks for viral replication. Another recent study reported the presence of actin
62 genes (viractins) in NCLDV genomes (Cunha et al., 2020). Viractins are hypothesized to
63 help viral infections by controlling the localization of the viral factory close to the host
64 nucleus.

65 Hundreds of genomes have already been sequenced for cultured NCLDV, yet
66 these represent only the tip of iceberg of the diverse NCLDV uncovered through
67 environmental surveys (Schulz et al., 2020). To by-pass cultivation, genome-resolved
68 metagenomics has been applied to large metagenomic surveys, including on oceanic
69 samples collected by *Tara* Oceans (Sunagawa et al., 2020), in order to characterize
70 NCLDV metagenome-assembled genomes (MAGs) containing the gene pool of thousands
71 of those viruses (Moniruzzaman et al., 2020; Schulz et al., 2020). NCLDV MAGs
72 revealed a cosmopolitan nature of these viruses, extensive gene transfers with eukaryotes,
73 and their complex metabolic capabilities.

74 In this study, we describe the identification of myosin genes in previously
75 published NCLDV MAGs as well as newly identified ones derived from a manual binning
76 and curation effort focused on large cellular size fractions of *Tara* Oceans enriched in
77 NCLDV when infecting planktonic eukaryotes (see Materials and Methods). Myosin
78 genes, which have not been previously described in viral genomes from cultures, form a
79 superfamily of motor proteins involved in a wide range of motility processes in eukaryotic
80 cells. Myosins have been grouped into various classes (Odroritz and Kollmar, 2007). Most
81 myosins are classified into class 1 to 35 based on their phylogenetic relationships (Odroritz
82 and Kollmar, 2007), whilst other myosins are phylogenetically orphan and classified into
83 class A to U (Odroritz and Kollmar, 2007). The functions of orphan myosins are often
84 unknown, while the functions of some members of the class 1 to 35 are characterized. For
85 example, some myosins of class 2 contract muscle (Pertici et al., 2018), whilst some
86 myosins of class 5 transport specific material along actin filaments (Hammer and Sellers,
87 2012). The various functions of myosins are supported by the head domains, which are
88 universally conserved among myosins, interact with actins, and frequently serve for
89 phylogenetic analyses. The head domains of myosins interact with actins when myosins
90 bind ADP, whereas, when ADP is absent or ATP is in the ADP-binding site of myosins, the
91 head domains no longer interact with actins.

92

93 **MATERIALS AND METHODS**

94 **NCLDV MAGs derived from the *Tara* Ocean Project**

95 Newly identified NCLDV metagenome-assembled genomes (MAGs) were manually

96 characterized and curated from the *Tara* Oceans metagenomes (size fractions > 0.8 μ m),
97 based on an initial binning strategy at large-scale focused on eukaryotes (Delmont et al.,
98 2020), and following the same workflow as in previous studies (Cunha et al., 2020; Kaneko
99 et al., 2020; Delmont et al., 2021). Briefly, metagenomes were organized into 11 sets based
100 on their geography, and each set was co-assembled using MEGAHIT (Li et al., 2015)
101 v.1.1.1. For each set, scaffolds longer than 2.5 kbp were processed within the
102 bioinformatics platform anvi'o v.6.1 (Eren et al., 2015) to generate genome-resolved
103 metagenomes (Delmont et al., 2018). CONCOCT (Alneberg et al., 2014) was used to
104 identify large clusters of contigs within the set. We then used HMMER (Eddy, 2011)
105 v3.1b2 to search for eight NCLDV gene markers (Guglielmini et al., 2019), and identified
106 NCLDV MAGs by manually binning CONCOCT clusters using the anvi'o interactive
107 interface. Finally, NCLDV MAGs were manually curated using the same interface, to
108 minimize contamination as described previously (Delmont and Eren, 2016).

109 **Sequence datasets**

110 To prepare a sequence set for the DNA polymerase elongation subunit family B (PolB),
111 we first extracted PolB sequences from NCVOG (Yutin et al., 2009). Next, we collected
112 PolB sequences by performing BLASTP from Virus-Host DB (Mihara et al., 2016) against
113 the PolB sequences from NCVOG. We retained hits with an E-value < 1e-10. To identify
114 PolBs in the NCLDV MAGs, we performed BALSTP from sequences derived from
115 NCDLV MAGs generated by Moniruzzaman et al. (Moniruzzaman et al., 2020), Schulz et
116 al. (Schulz et al., 2020) and ourselves (*Tara* Oceans MAGs) against the PolB sequences
117 from NCVOG and Virus-Host DB. We retained hits with an E-value < 1e-10 and with their
118 length in a range from 800 amino acids (aa) up to 1800 aa. We pooled these PolB sequences,
119 and then removed redundancy using cd-hit (4.8.1) (Li and Godzik, 2006) and manually
120 curated the dataset to reduce its size.

121 For myosin homologs, we used full-length myosin sequences from a previous
122 study (Odroritz and Kollmar, 2007) as primal references for myosins. This dataset contains
123 various classes of myosins from diverse organisms. Next, we extracted myosin homologs
124 from MMETSP (Keeling et al., 2014) and RefSeq (O'Leary et al., 2016) by performing
125 BLASTP (blast 2.11.0) against the primal references to generate secondary references for
126 full-length myosin sequences. We considered hits with an E-value < 1e-10 in this search.
127 We identified myosin head domains in the primal and secondary myosin reference

128 sequences by performing hmmscan (HMMER 3.3.1) (Eddy, 2011). We used Pfam (El-
129 Gebali et al., 2019) as the HMM model for the hmmscan search and considered hits that
130 were annotated as “Myosin_head” and showed an E-value < 1e-10. We filtered out the
131 primal and secondary reference sequences to reduce redundant sequences. To identify
132 myosin sequences in the NCLDV MAGs, we performed BLASTP from sequences derived
133 from MAGs against the primal myosin references. We considered hits with an E-value <
134 1e-10. We identified myosin head domains by performing hmmscan (Eddy, 2011). We
135 considered hits that were annotated as “Myosin_head” with an E-value < 1e-10 and length
136 longer than 550 aa and shorter than 800 aa.

137 **Multiple sequence alignment**

138 Multiple sequence alignments were generated using MAFFT (v7.471) (Katoh et al., 2019)
139 with the L-INS-i algorithm, which is suitable for sequences that have only one alignable
140 domain. After multiple alignment, we removed gappy sites by using trimal (v1.4.rev15)
141 (Capella-Gutiérrez et al., 2009) with “-gappyout” option.

142 For myosin sequences from viruses and eukaryotes, we generated two trimmed
143 alignments by removing gapped columns using “-strict” option (named “strict dataset”),
144 in addition to the “-gappyout” option (named “gappy dataset”). Finally, we removed
145 sequences which have more than 30% gaps along the entire length of the alignment from
146 each dataset.

147 **Phylogenetic analysis**

148 The phylogenetic analyses were conducted with the ML framework using IQ-TREE
149 (1.6.12) (Minh et al., 2020). For each alignment, we used the best substitution model
150 selected by IQ-TREE. The selected models are described in the figure legends. The branch
151 support values were computed based on non-parametric bootstrap method with 100
152 bootstrap replicates.

153 For myosin sequences from viruses and eukaryotes, we also built phylogenetic
154 trees using RAxML (8.2.12) (Stamatakis, 2014) on both “gappy” and “strict” datasets.
155 Therefore, we obtained four trees for these myosin sequences (i.e., gappy/IQ-TREE,
156 strict/IQ-TREE, gappy/RAxML, and strict/RAxML).

157 **Visualization**

158 The phylogenetic trees were visualized with iTOL v4 (Letunic and Bork, 2019).

159 **Statistical test for co-existing genes**

160 We performed InterProScan (5.44-79.0) (Mitchell et al., 2019) to find motifs against each
161 protein sequence derived from the NCLDV MAGs. We counted the number of each motif
162 discovered in *Imitervirales*, which was annotated based on the PolB phylogenetic tree.
163 Next, we conducted chi-square test with the Benjamini-Hochberg correction to set the false
164 discovery rate at 0.01 to define the motifs that were significantly enriched in the
165 *Imitervirales* encoding virmyosins compared with other *Imitervirales*.

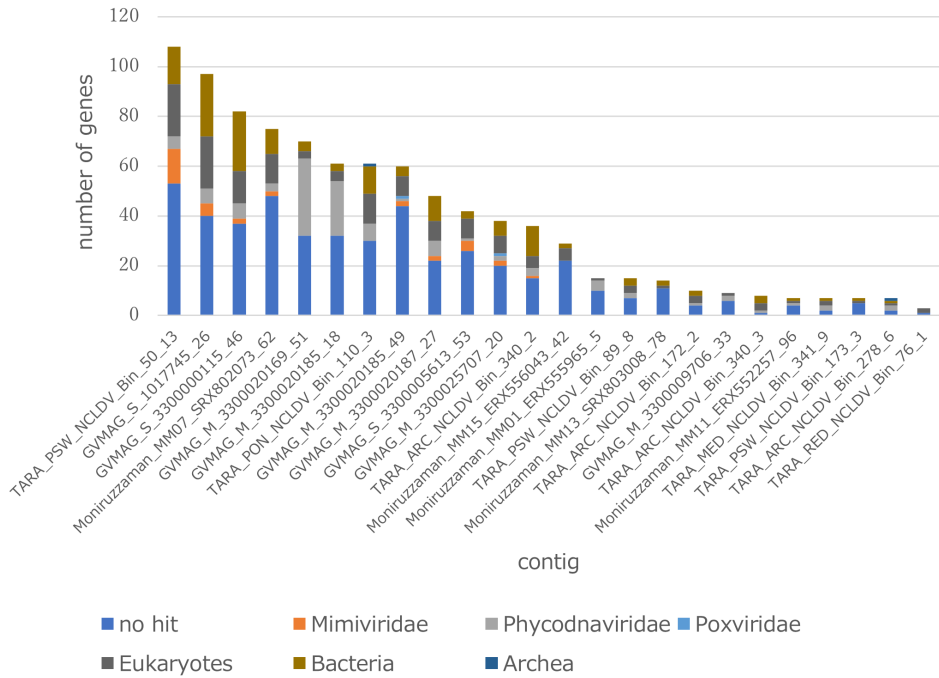
166

167 **RESULTS AND DISCUSSION**

168 **Myosin genes in NCLDV genomes**

169 We identified myosin-related genes in a total of 24 NCLDV MAGs (out of 2,275
170 considered in our survey) by performing BLASTP against reference myosin sequences
171 compiled from a previous study (Odroritz and Kollmar, 2007), through our own effort
172 independent from a parallel environmental genomic survey (Ha et al., 2021). These
173 NCLDV MAGs were derived from the large cellular size fractions of *Tara Oceans* (n=10)
174 and studies by Moniruzzaman et al. (n=5) and Schulz et al. (n=9) (Moniruzzaman et al.,
175 2020; Schulz et al., 2020). All NCLDV MAGs but one originate from marine plankton
176 samples (**Table S1**). The viral sequences contain the head domain but do not show the tail
177 domain. An alignment of myosin head domain sequences from various organisms with
178 these viral sequences establishes their strong homology (**Figure S1**). The taxonomies of
179 the closest homologs of other genes encoded together with the myosin homologs in the
180 same contigs (**Figure 1**) revealed that a large proportion of genes (up to 44% and 15% on
181 average) in the contigs best match to NCLDV genes, thus excluding the possibility of
182 contaminated myosin homologs in the NCLDV MAGs. We designate the viral myosin
183 homologs as virmyosins.

184



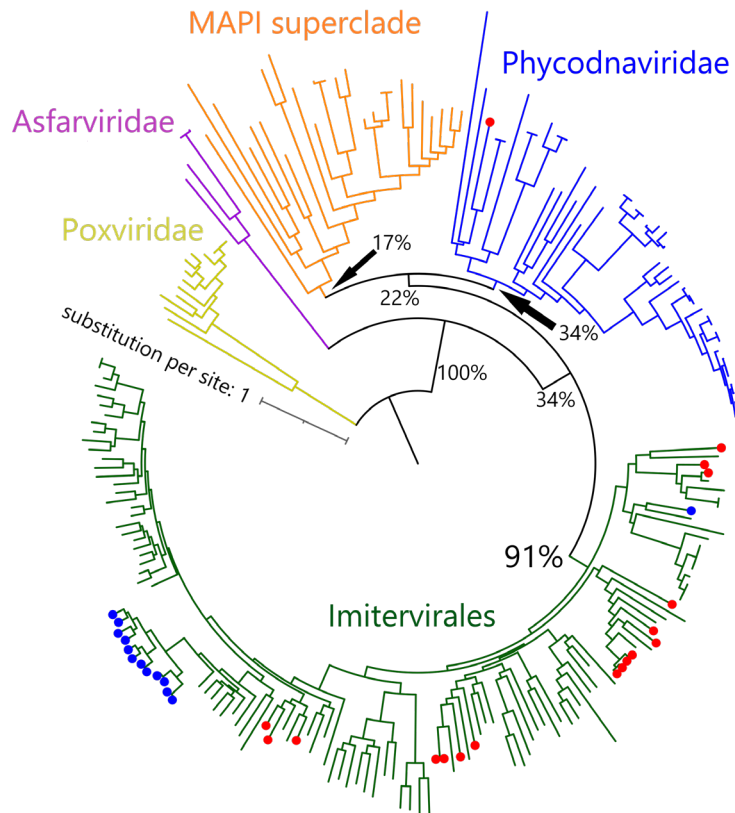
185

186 **Figure 1.** Taxonomic annotation of genes encoded in the virmyosin-harboring NCLDV contigs. Best
187 hit-based taxonomic annotation was performed for each gene using BLAST against the RefSeq
188 database.

189

190 To investigate the evolutionary relationships between the virmyosin-encoding
191 NCLDVs, we performed phylogenetic analyses based on DNA polymerases (PolBs), a
192 commonly used phylogenetic marker for NCLDVs. Eighteen of the 24 virmyosin-harboring
193 MAGs were found to also encode PolB and were thus subjected to this analysis. The
194 generated tree indicates that all but one of these virmyosin-encoding MAGs belong to the
195 *Imitervirales* order, the grouping of which was supported with a bootstrap value of 91%
196 (**Figure 2**). However, the lineages of virmyosin-encoding MAGs were scattered within at
197 least four clades of the *Imitervirales* branches. The *Imitervirales* MAGs previously shown
198 to encode viractins did not show close relationships with the virmyosin encoding MAGs.
199 One of the virmyosin-encoding MAGs was identified within the *Phycodnaviridae* family.

200



201

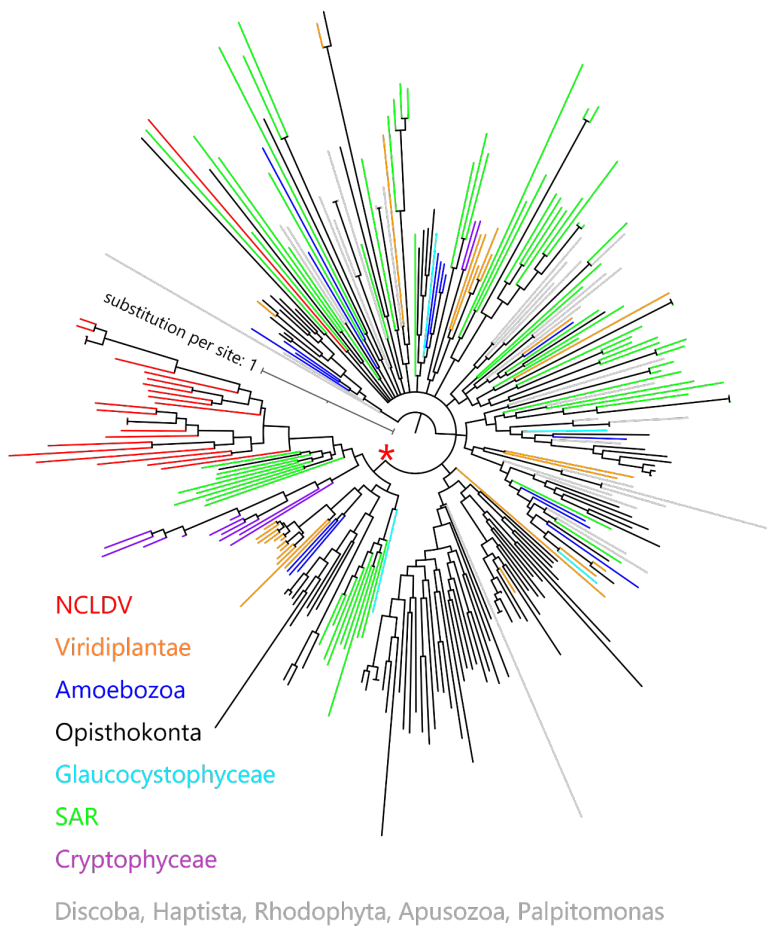
202 **Figure 2.** Phylogenetic tree of NCLDVs based on DNA polymerase B. The tree was built from 219
203 PolB sequences of NCLDVs (18 MAGs encoding myosin gene, 13 MAGs encoding actin gene, and
204 188 other broad and unbiased taxa from the reference database). Branches labeled with red and
205 blue circles represent NCLDV MAGs with virmyosin and viractin genes, respectively. Branches are
206 color-coded based on family- or order-level taxonomy. The MAPI superclade (shown in orange)
207 comprises *Marseilleviridae*, *Ascoviridae*, Pitho-like viruses and *Iridoviridae*. The bootstrap value
208 for the branch between *Imitervirales* and other families is 91%. We used *Poxviridae* as an
209 outgroup to root the tree. The LG+F+R10 substitution model was selected by IQ-TREE for the best
210 model for tree reconstruction.

211

212 Since myosins are universal in the eukaryotic domain, we hypothesized that these
213 NCLDVs acquired myosin homologs by horizontal gene transfers (HGTs) from various
214 eukaryotes. To determine the source eukaryotic lineages for the putative HGTs, we
215 performed phylogenetic analyses on the virmyosin and reference myosin sequences. We

216 generated four phylogenetic trees with different methods (**Figure 3**, **Figure S2**, see
217 Materials and Methods). The phylogenetic placement of the virmyosin from the MAG
218 belonging to the *Phycodnaviridae* family was unstable. However, all the trees showed a
219 monophyletic group of *Imitervirales* virmyosins. The grouping is supported by a bootstrap
220 value of 71% (**Figure S2a**).

221



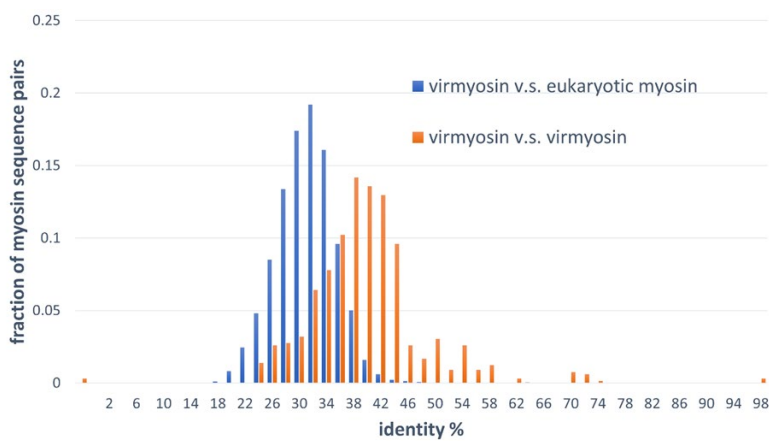
222

223 **Figure 3.** Phylogeny of myosin from NCLDVs and eukaryotic lineages. The tree was built from the
224 multiple sequence alignment of 286 myosin head domain sequences. Branches are color-coded
225 based on taxonomic groups (red branches correspond to virmyosins). We consider myosin-II as an
226 outgroup to root this tree. The LG+R10 substitution model was selected by IQ-TREE for the best
227 model for tree reconstruction.

228

229 To examine the effect of long-branch attraction on the formation of the
230 *Imitervirales* virmyosin clade, we computed the pair-wise sequence identities within
231 virmyosins and between virmyosins and eukaryotic myosins (Figure 4). The sequence
232 similarities for many of the virmyosin pairs were higher than those between virmyosins
233 and eukaryotic myosins, thus diminishing the possibility of long branch attraction effect
234 on the monophyletic grouping the *Imitervirales* virmyosins. The *Imitervirales* virmyosin
235 clade is branching out from orphan myosins of the SAR (Stramenopiles, Alveolates, and
236 Rhizaria) supergroup, but the grouping of these virmyosins and the orphan myosins was
237 not supported. Finally, to further improve the tree reconstruction, we built a phylogenetic
238 tree using the virmyosin sequences as well as eukaryotic myosin sequences that formed a
239 clade together with the virmyosins (the clade marked with '*' in Figure 3). The newly
240 generated tree again displayed the monophyletic grouping of the *Imitervirales* virmyosins
241 (bootstrap value, 98%) and placed it within a clade of myosin sequences from
242 Stramenopiles (the diatom *Thalassiosira pseudonana*, and the oomycete
243 *Hyaloperonospora parasitica*) and a fungus (*Rhizopogon burlinghamii*) (Figure 5, Figure
244 S2e). The grouping between the virmyosins and the eukaryotic myosins was not supported
245 (bootstrap value, 15%), leaving the origin of the vimyosins unresolved.

246

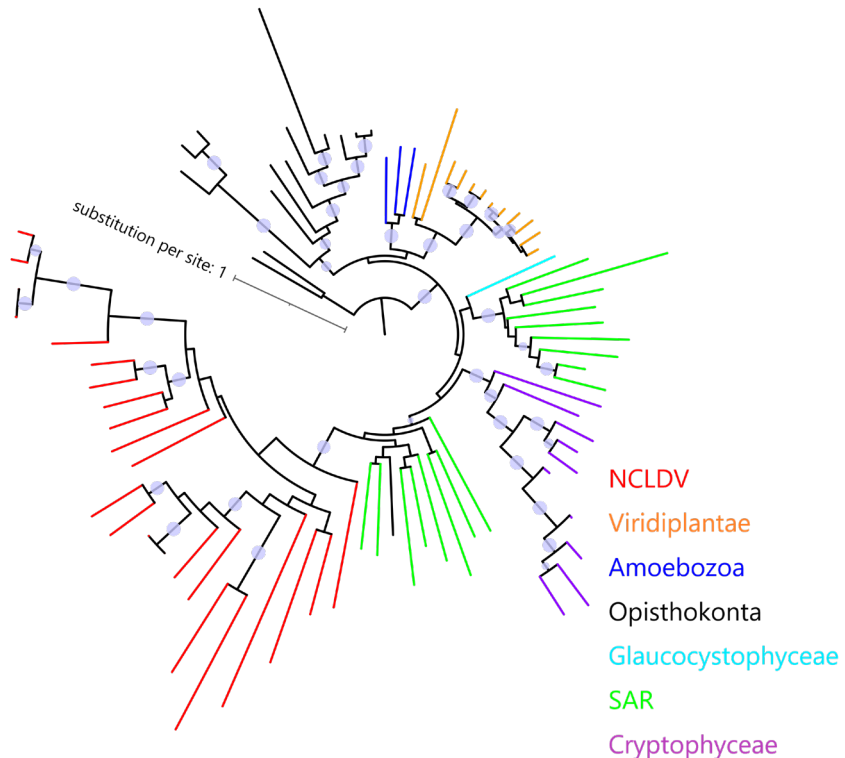


247

248 **Figure 4.** Distributions of pair-wise myosin sequence similarities within the NCLDV (virmyosin vs
249 virmyosin) and between NCLDV and eukaryotes (virmyosin vs eukaryotic myosin). This graph

250 shows that the mean value of myosin similarity within NCLDVs is higher than that between
251 NCLDVs and eukaryotes.

252



254 **Figure 5.** Phylogeny of virmyosins and their close relatives in eukaryotes. The tree was built from
255 81 myosin sequences of NCLDVs, Amoebozoa, SAR, Opisthokonta, Cryptophyceae, Viridiplantae
256 and Glaucocystophyceae. Branches are color-coded based on taxonomic groups (red branches
257 correspond to virmyosins). We consider myosin-II of *Nasonia vitripennis* and *Neurospora crassa*
258 as outgroups to root this tree. Bootstrap values higher than 80% are represented as circles on the
259 branches. The LG+F+R7 substitution model was selected by IQ-TREE for the best model for tree
260 reconstruction.

261

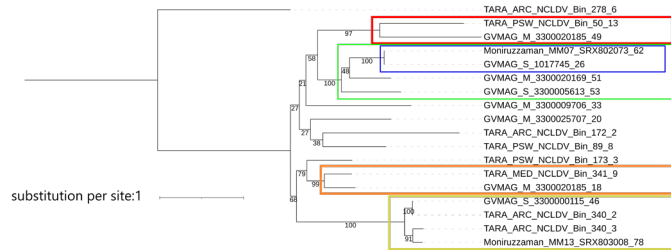
262 Incongruence of phylogenetic trees between myosins and DNA polymerases

263 We next examined the congruence of the virmyosin and PolB trees by focusing on the 18
264 virmyosins that were found in MAGs that encode PolB. Congruence of the topologies

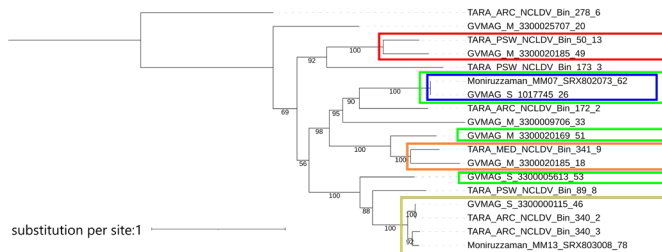
265 between these trees is expected if the original virmyosin gene was acquired by an ancestral
266 virus prior to the divergence of viral clades or families. We generated a new phylogenetic
267 tree based on the 18 virmyosin sequences and the 18 PolB sequences. To investigate the
268 congruence of the trees, we focused on clades in the virmyosin tree that were supported
269 with a bootstrap value greater than 90% (Figure 6). The analysis revealed that several
270 groups of closely related sequences [i.e., (TARA_PSW_NCLDV_Bin_50_13,
271 GVMAG_M_3300020185_49); (Moniruzzaman_MM07_SRX802073_62,
272 GVMAG_S_1017745_26); (TARA_MED_NCLDV_Bin_341_9,
273 GVMAG_M_3300020185_18); (GVMAG_S_3300000115_46,
274 TARA_ARC_NCLDV_Bin_340_2, (TARA_ARC_NCLDV_Bin_340_3,
275 Moniruzzaman_MM13_SRX803008_78)] form monophyletic groups also in the PolB tree.
276 However, these two trees were incongruent at deeper branches. For instance, one of the
277 monophyletic clades in the virmyosin tree composed of four MAGs [i.e.,
278 (Moniruzzaman_MM07_SRX802073_62, GVMAG_S_1017745_26,
279 GVMAG_M_3300020169_51, GVMAG_S_3300005613_53)] turned out to be
280 polyphyletic with statistical supports in the PolB tree (Figure 6). This result suggests that
281 multiple and distantly related ancestral viruses of *Imitervirales* independently acquired
282 myosin genes through HGTs.

283

a) Phylogenetic tree of myosin



b) Phylogenetic tree of PolB



284

285 **Figure 6.** Phylogenetic trees of (a) myosin and (b) PolB sequences from MAGs encoding both genes.
286 Labels at the leaves are the identifiers of the NCLDV MAGs. Clades supported with a bootstrap
287 value >90% in the myosin tree are marked in both trees by colored rectangles. The LG+F+I+G4
288 substitution model was selected by IQ-TREE for the best model for both tree reconstructions.

289

290 The monophyletic grouping of the *Imitervirales* virmyosins and the scattered
291 distribution of the virmyosin-encoding *Imitervirales* in the PolB tree are intriguing. We
292 consider three major possibilities for the origin of virmyosins. The first possibility is that
293 all the *Imitervirales* myosin genes were vertically inherited from an ancestral virus of the
294 *Imitervirales*, and subsequently lost independently in most of the descendant lineages. This
295 scenario is not parsimonious as it assumes many independent gene losses. The second
296 possibility is that myosin genes were independently recruited multiple times from
297 eukaryotes by ancestral viruses belonging to the *Imitervirales*. This scenario can account
298 for the topological differences in the two trees. However, this scenario cannot readily
299 explain the monophyletic grouping of the virmyosins, as this scenario needs to additionally
300 assume independent horizontal acquisitions of myosin genes by distantly related ancestral
301 viruses from the same or closely related eukaryotes (e.g., ancestral Stramenopiles). Such
302 acquisitions seem implausible because host changes are likely rampant events for

303 *Imitervirales* given the wide host ranges of the known viruses in this group (Sun et al.,
304 2020). The third possibility is that a myosin gene transfer occurred once in a viral lineage
305 of *Imitervirales* from its host. Then, after the viral myosin gene acquired beneficial
306 functions for the virus, this gene was transferred to other viruses, probably during co-
307 infection in the same host (which may be different from the current hosts). Of note, a
308 previous study reported a clear case of horizontal gene transfer between NCLDVs
309 (Christo-Foroux et al., 2020). This last scenario can explain both the topological difference
310 between the virmyosin and PolB trees and the monophyletic grouping of the virmyosins.
311 Further exploration of the actual diversity of *Imitervirales*, and more globally of NCLDVs,
312 from various environments will certainly provide important insights regarding the
313 robustness of these hypotheses

314 **Kinesin genes are associated with virmyosin genes**

315 We identified 880 protein families/domains that showed a significant level of co-
316 occurrence with virmyosin genes among the MAGs of the *Imitervirales* order by
317 performing chi-square test (false discovery rate 0.01; **Table S2**). Interestingly, kinesins
318 were significantly enriched in the *Imitervirales* MAGs encoding virmyosin (q -value =
319 2.9e-33, ranked at 7-th). Of 24 MAGs encoding virmyosins, 16 (67%) encoded kinesins,
320 a score that might be underestimated due to the possible incomplete nature of NCLDV
321 MAGs. Myosins are known to walk along actin filaments, which are located at the
322 peripheric side of the cytoplasm, whilst kinesins walk toward the outer side of the
323 cytoplasm along microtubules, which are mainly located in the inner side of the cytoplasm.
324 Both kinesins and some classes of myosins function as a transporter to carry specific
325 materials on these filaments. Viral kinesins may function to transport viral particles along
326 microtubules and pass them to viral myosins at the end of microtubules. Myosins then
327 transport viruses to the outer side of the cell to finally export the viral particles outside the
328 cell. Intracellular enveloped viruses of vaccinia virus are transported towards the cell
329 surface in a microtubule-dependent process (Hollinshead et al., 2001). It is possible that
330 the viral myosins and kinesins found in NCLDV MAGs may function in a similar viral
331 particle transport process.

332 **CONCLUSIONS**

333 In this study, we provided strong evidence showing that marine members of NCLDVs

334 encode myosin homologs (virmyosins), which contain the head domain but lack the tail
335 domain. The function of virmyosin could not be inferred based on the similarity to
336 functionally characterized myosin homologs. However, virmyosin genes were frequently
337 accompanied by kinesin genes, another class of motor proteins widespread in the
338 eukaryotic domain. Together with the previously discovered actin homologs in NCLDVs,
339 these results suggest that the genetic independence of NCLDVs from their hosts
340 encompasses a wide-range of cellular processes, including intracellular trafficking as
341 implied by our study and the translation process as considered from previous discoveries
342 of translation genes in this group of viruses. Our phylogenetic analyses suggest a complex
343 evolutionary origin of the virmyosin genes, which may involve not only HGTs from
344 eukaryotes to NCLDVs but also intra-virus HGTs within NCLDVs. The functions encoded
345 in the huge genetic pool of NCLDVs are revealing the amazingly diverse strategies to
346 control host cellular processes in this diverse group of viruses. Scrutinizing available and
347 newly generated environmental genomes will contribute to better characterizing the
348 infection strategies of this fascinating group of viruses.

349 **ACKNOWLEDGEMENTS**

350 This study was supported by JSPS KAKANHI (18H02279) and Research Unit for
351 Development of Global Sustainability, Kyoto University Research Coordination Alliance.
352 Computation time was provided by the SuperComputer System, Institute for Chemical
353 Research, Kyoto University.

354

355 **REFERENCES**

356 Abergel, C., Legendre, M., and Claverie, J.-M. (2015). The rapidly expanding universe
357 of giant viruses: Mimivirus, Pandoravirus, Pithovirus and Mollivirus. *FEMS
358 Microbiol. Rev.* 39, 779–796. doi:10.1093/femsre/fuv037.

359 Alneberg, J., Bjarnason, B. S., de Bruijn, I., Schirmer, M., Quick, J., Ijaz, U. Z., et al.
360 (2014). Binning metagenomic contigs by coverage and composition. *Nat.
361 Methods* 11, 1144–1146. doi:10.1038/nmeth.3103.

362 Blanc-Mathieu, R., Dahle, H., Hofgaard, A., Brandt, D., Ban, H., Kalinowski, J., et al.
363 (2021). A persistent giant algal virus, with a unique morphology, encodes an
364 unprecedented number of genes involved in energy metabolism. *J. Virol.*
365 doi:10.1128/JVI.02446-20.

366 Capella-Gutiérrez, S., Silla-Martínez, J. M., and Gabaldón, T. (2009). trimAl: a tool for
367 automated alignment trimming in large-scale phylogenetic analyses.
368 *Bioinformatics* 25, 1972–1973. doi:10.1093/bioinformatics/btp348.

369 Christo-Foroux, E., Alempic, J.-M., Lartigue, A., Santini, S., Labadie, K., Legendre, M.,
370 et al. (2020). Characterization of Mollivirus kamchatka, the First Modern
371 Representative of the Proposed Molliviridae Family of Giant Viruses. *J. Virol.*
372 94. doi:10.1128/JVI.01997-19.

373 Colson, P., La Scola, B., and Raoult, D. (2017). Giant Viruses of Amoebae: A Journey
374 Through Innovative Research and Paradigm Changes. *Annu. Rev. Virol.* 4, 61–
375 85. doi:10.1146/annurev-virology-101416-041816.

- 376 Cunha, V. D., Gaia, M., Ogata, H., Jaillon, O., Delmont, T. O., and Forterre, P. (2020).
377 Giant viruses encode novel types of actins possibly related to the origin of
378 eukaryotic actin: the viractins. *Evolutionary Biology*
379 doi:10.1101/2020.06.16.150565.
- 380 Delmont, T. O., and Eren, A. M. (2016). Identifying contamination with advanced
381 visualization and analysis practices: metagenomic approaches for eukaryotic
382 genome assemblies. *PeerJ* 4, e1839. doi:10.7717/peerj.1839.
- 383 Delmont, T. O., Gaia, M., Hinsinger, D. D., Fremont, P., Vanni, C., Guerra, A. F., et al.
384 (2021). Functional repertoire convergence of distantly related eukaryotic
385 plankton lineages revealed by genome-resolved metagenomics. *bioRxiv*,
386 2020.10.15.341214. doi:10.1101/2020.10.15.341214.
- 387 Delmont, T. O., Quince, C., Shaiber, A., Esen, Ö. C., Lee, S. T., Rappé, M. S., et al.
388 (2018). Nitrogen-fixing populations of Planctomycetes and Proteobacteria are
389 abundant in surface ocean metagenomes. *Nat. Microbiol.* 3, 804–813.
390 doi:10.1038/s41564-018-0176-9.
- 391 Eddy, S. R. (2011). Accelerated Profile HMM Searches. *PLOS Comput. Biol.* 7,
392 e1002195. doi:10.1371/journal.pcbi.1002195.
- 393 El-Gebali, S., Mistry, J., Bateman, A., Eddy, S. R., Luciani, A., Potter, S. C., et al. (2019).
394 The Pfam protein families database in 2019. *Nucleic Acids Res.* 47, D427–D432.
395 doi:10.1093/nar/gky995.
- 396 Eren, A. M., Esen, Ö. C., Quince, C., Vineis, J. H., Morrison, H. G., Sogin, M. L., et al.
397 (2015). Anvi’o: an advanced analysis and visualization platform for ‘omics data.
398 *PeerJ* 3. doi:10.7717/peerj.1319.
- 399 Guglielmini, J., Woo, A. C., Krupovic, M., Forterre, P., and Gaia, M. (2019).
400 Diversification of giant and large eukaryotic dsDNA viruses predated the origin
401 of modern eukaryotes. *Proc. Natl. Acad. Sci.* 116, 19585–19592.
402 doi:10.1073/pnas.1912006116.

- 403 Ha, A. D., Moniruzzaman, M., and Aylward, F. O. (2021). High Transcriptional Activity
404 and Diverse Functional Repertoires of Hundreds of Giant Viruses in a Coastal
405 Marine System. *bioRxiv*, 2021.03.08.434518. doi:10.1101/2021.03.08.434518.
- 406 Hammer, J. A., and Sellers, J. R. (2012). Walking to work: roles for class V myosins as
407 cargo transporters. *Nat. Rev. Mol. Cell Biol.* 13, 13–26. doi:10.1038/nrm3248.
- 408 Hollinshead, M., Rodger, G., Van Eijl, H., Law, M., Hollinshead, R., Vaux, D. J. T., et
409 al. (2001). Vaccinia virus utilizes microtubules for movement to the cell surface.
410 *J. Cell Biol.* 154, 389–402. doi:10.1083/jcb.200104124.
- 411 Iyer, L. M., Balaji, S., Koonin, E. V., and Aravind, L. (2006). Evolutionary genomics of
412 nucleo-cytoplasmic large DNA viruses. *Virus Res.* 117, 156–184.
413 doi:10.1016/j.virusres.2006.01.009.
- 414 Kaneko, H., Blanc-Mathieu, R., Endo, H., Chaffron, S., Delmont, T. O., Gaia, M., et al.
415 (2020). Eukaryotic virus composition can predict the efficiency of carbon export
416 in the global ocean. *iScience* 24. doi:10.1016/j.isci.2020.102002.
- 417 Katoh, K., Rozewicki, J., and Yamada, K. D. (2019). MAFFT online service: multiple
418 sequence alignment, interactive sequence choice and visualization. *Brief.
419 Bioinform.* 20, 1160–1166. doi:10.1093/bib/bbx108.
- 420 Keeling, P. J., Burki, F., Wilcox, H. M., Allam, B., Allen, E. E., Amaral-Zettler, L. A., et
421 al. (2014). The Marine Microbial Eukaryote Transcriptome Sequencing Project
422 (MMETSP): Illuminating the Functional Diversity of Eukaryotic Life in the
423 Oceans through Transcriptome Sequencing. *PLOS Biol.* 12, e1001889.
424 doi:10.1371/journal.pbio.1001889.
- 425 Koonin, E. V., Dolja, V. V., Krupovic, M., Varsani, A., Wolf, Y. I., Yutin, N., et al. (2020).
426 Global Organization and Proposed Megataxonomy of the Virus World.
427 *Microbiol. Mol. Biol. Rev. MMBR* 84. doi:10.1128/MMBR.00061-19.
- 428 Koonin, E. V., and Yutin, N. (2019). “Chapter Five - Evolution of the Large
429 Nucleocytoplasmic DNA Viruses of Eukaryotes and Convergent Origins of Viral

- 430 Gigantism,” in *Advances in Virus Research*, eds. M. Kielian, T. C. Mettenleiter,
431 and M. J. Roossinck (Academic Press), 167–202.
432 doi:10.1016/bs.aivir.2018.09.002.
- 433 Letunic, I., and Bork, P. (2019). Interactive Tree Of Life (iTOL) v4: recent updates and
434 new developments. *Nucleic Acids Res.* 47, W256–W259.
435 doi:10.1093/nar/gkz239.
- 436 Li, D., Liu, C.-M., Luo, R., Sadakane, K., and Lam, T.-W. (2015). MEGAHIT: an ultra-
437 fast single-node solution for large and complex metagenomics assembly via
438 succinct de Bruijn graph. *Bioinformatics* 31, 1674–1676.
439 doi:10.1093/bioinformatics/btv033.
- 440 Li, W., and Godzik, A. (2006). Cd-hit: a fast program for clustering and comparing large
441 sets of protein or nucleotide sequences. *Bioinformatics* 22, 1658–1659.
442 doi:10.1093/bioinformatics/btl158.
- 443 Mihara, T., Nishimura, Y., Shimizu, Y., Nishiyama, H., Yoshikawa, G., Uehara, H., et al.
444 (2016). Linking Virus Genomes with Host Taxonomy. *Viruses* 8, 66.
445 doi:10.3390/v8030066.
- 446 Minh, B. Q., Schmidt, H. A., Chernomor, O., Schrempf, D., Woodhams, M. D., von
447 Haeseler, A., et al. (2020). IQ-TREE 2: New Models and Efficient Methods for
448 Phylogenetic Inference in the Genomic Era. *Mol. Biol. Evol.* 37, 1530–1534.
449 doi:10.1093/molbev/msaa015.
- 450 Mitchell, A. L., Attwood, T. K., Babbitt, P. C., Blum, M., Bork, P., Bridge, A., et al.
451 (2019). InterPro in 2019: improving coverage, classification and access to
452 protein sequence annotations. *Nucleic Acids Res.* 47, D351–D360.
453 doi:10.1093/nar/gky1100.
- 454 Moniruzzaman, M., Martinez-Gutierrez, C. A., Weinheimer, A. R., and Aylward, F. O.
455 (2020). Dynamic genome evolution and complex virocell metabolism of
456 globally-distributed giant viruses. *Nat. Commun.* 11, 1710. doi:10.1038/s41467-
457 020-15507-2.

- 458 Odronitz, F., and Kollmar, M. (2007). Drawing the tree of eukaryotic life based on the
459 analysis of 2,269 manually annotated myosins from 328 species. *Genome Biol.*
460 8, R196. doi:10.1186/gb-2007-8-9-r196.
- 461 O'Leary, N. A., Wright, M. W., Brister, J. R., Ciufo, S., Haddad, D., McVeigh, R., et al.
462 (2016). Reference sequence (RefSeq) database at NCBI: current status,
463 taxonomic expansion, and functional annotation. *Nucleic Acids Res.* 44, D733–
464 D745. doi:10.1093/nar/gkv1189.
- 465 Pertici, I., Bongini, L., Melli, L., Bianchi, G., Salvi, L., Falorsi, G., et al. (2018). A
466 myosin II nanomachine mimicking the striated muscle. *Nat. Commun.* 9.
467 doi:10.1038/s41467-018-06073-9.
- 468 Schulz, F., Roux, S., Paez-Espino, D., Jungbluth, S., Walsh, D. A., Denef, V. J., et al.
469 (2020). Giant virus diversity and host interactions through global metagenomics.
470 *Nature* 578, 432–436. doi:10.1038/s41586-020-1957-x.
- 471 Scola, B. L., Audic, S., Robert, C., Jungang, L., Lamballerie, X. de, Drancourt, M., et
472 al. (2003). A Giant Virus in Amoebae. *Science* 299, 2033–2033.
473 doi:10.1126/science.1081867.
- 474 Stamatakis, A. (2014). RAxML version 8: a tool for phylogenetic analysis and post-
475 analysis of large phylogenies. *Bioinformatics* 30, 1312–1313.
476 doi:10.1093/bioinformatics/btu033.
- 477 Sun, T.-W., Yang, C.-L., Kao, T.-T., Wang, T.-H., Lai, M.-W., and Ku, C. (2020). Host
478 Range and Coding Potential of Eukaryotic Giant Viruses. *Viruses* 12.
479 doi:10.3390/v12111337.
- 480 Sunagawa, S., Acinas, S. G., Bork, P., Bowler, C., Eveillard, D., Gorsky, G., et al. (2020).
481 Tara Oceans: towards global ocean ecosystems biology. *Nat. Rev. Microbiol.* 18,
482 428–445. doi:10.1038/s41579-020-0364-5.
- 483 Yutin, N., Wolf, Y. I., Raoult, D., and Koonin, E. V. (2009). Eukaryotic large nucleo-
484 cytoplasmic DNA viruses: Clusters of orthologous genes and reconstruction of

485 viral genome evolution. *Virol. J.* 6, 223. doi:10.1186/1743-422X-6-223.

486